Automated Segmentation of Tumours in MRI Brain Scans

Ali M. Hasan[1,2], Farid Meziane[2] and Mohammad Abd Kadhim[1]
[1]College of Medicine, Al-Nahrain University, Baghdad, Iraq
[2]School of Computing, Science and Engineering, University of Salford, Manchester, U.K.

Keywords: Magnetic Resonance Scanning, Bounding 3D Box based Genetic Algorithm, Mid-Sagittal Plane, Principal Components Analysis.

Abstract: The research reported in this paper concerns the development of a novel automated algorithm to identify and segment brain tumours in MRI scans. The input is the patient's scan slices and the output is a subset of the slices that includes the tumour. The proposed method is called Bounding 3D Box Based Genetic Algorithm (BBBGA) and is based on the use of Genetic Algorithm (GA) to search for the most dissimilar regions between the left and right hemispheres of the brain. The process involves randomly generating a hundred of 3D boxes with different sizes and locations in the left hemisphere of the brain and compared with the corresponding 3D boxes in the right hemisphere of the brain through the objective function. These 3D boxes are moved and updated during the iterations of the GA towards the region of maximum dissimilarity between the two hemispheres which represent the approximate position of the tumour. The dataset includes 88 pathological patients provided by the MRI Unit of Al-Kadhimiya Teaching Hospital in Iraq. The achieved accuracy of the BBBGA and 3D segmentation of the tumour were 95% and 90% respectively.

1 INTRODUCTION

Medical image processing expanded dramatically during the last decade and became a popular research field that attracted interests from various fields such as mathematics, computer science, engineering, biology and medicine with applications in clinical practice and biomedical imaging to examine and support diagnoses and therapy in human patients. An important stage of medical image processing is segmentation which is seen as a complex and challenging process, particularly with brain images due to the nature of the images. Indeed, the brain has a complicated structure and more accurate segmentation is essential for detecting tumours, edema in order to describe therapy (Shen et al., 2005). The edema associates with intracranial brain tumours and is the result of leakage of plasma into the parenchyma through dysfunctional cerebral capillaries (Kaal and Vecht, 2004).

Many works reported in the literature attempted to detect and classify brain tumours. Saha et al., (2002), proposed an automated brain tumour and edema algorithm to implement fast segmentation of MRI brain scanning images based on the bounding boxes method. The Bhattacharya coefficient of grey scale intensity histograms was used as a score function that locates bounding boxes around the abnormal area in the MRI slice. This method was used to search in a parallel way for the most dissimilar region in an MRI brain scan between the left and right hemispheres in an axial view of the MRI (Ray et al., 2008).

Khandani et al. (2009) proposed an automated algorithm for detecting tumour location in MRI brain images and identified the tumour boundary by using an unsupervised learning algorithm called Force algorithm. A set of prior operations such as skull removal, non-tumour pixels removal by using histogram analysis and exponential transformation was first implemented. The tumour area was then segmented using histogram thresholding.

Bauer et al., (2011) developed an automated algorithm to delineate the boundary of the brain tumour by combining Support Vector Machine (SVM) classifier and subsequent hierarchical regularization based on Conditional Random Fields (CRF). SVM was also used by Mikulka and Gescheidtov (2013) in a segmentation method to recognize brain tumour, edema and necrosis in T1 and T2 MRI weighted images.

Nabizadeh and Kubat (2015) developed a fully automated algorithm for brain tumours recognition

Hasan, A., Meziane, F. and Kadhim, M.
Automated Segmentation of Tumours in MRI Brain Scans.
DOI: 10.5220/0005625900550062
In *Proceedings of the 9th International Joint Conference on Biomedical Engineering Systems and Technologies (BIOSTEC 2016) - Volume 2: BIOIMAGING*, pages 55-62
ISBN: 978-989-758-170-0

and segmentation in MRI by using five effective texture-based statistical feature extraction methods namely first order statistical features, Grey Level Co-occurrence Matrix (GLCM), Grey Level Run Length Matrix (GLRLM), histogram of oriented gradient HOG and linear binary pattern (LBP).

We addressed the above-mentioned shortcomings, by developing an algorithm that is:

1. Independent of atlas registration in order to avoid any inaccurate registration process that affects the measurement of the tumours' classification (Nabizadeh and Kubat, 2015).
2. Fully automated with no human intervention or initialization.

The rest of this paper is organized as follows. In Section 2, material and methods are described and the BBBGA method is explained in details in section 3. In section 4, tumour segmentation by 3D Active Contour without Edge method is explained and experimental results are given in Section 5. The conclusion is drawn in Section 6.

2 MATERIAL AND METHODS

The main objective of this research is to develop and evaluate an automated algorithm for identifying the location of tumours in MRI brain slices as well as identifying the most important slices of pathological patient to draw the attention of the clinicians to these slices. The overall flow chart of the proposed algorithm is shown in Fig. 1. It starts with the data collection step from the Iraqi hospital, a set of algorithms in the pre-processing stage and finally the segmentation algorithm.

2.1 MRI Acquisition

Data collection is an important steps in this study. T2 and T1 weighted images of 88 pathological patients were collected from the MRI Unit of Al Kadhimiya Teaching Hospital in Iraq.

Each patient has 32 slices with a slice resolution of (432×512 pixels), the inter-slice spacing is 5.5 mm, and slice thickness is 5 mm. The MRI Unit in the mentioned hospital has faced many problems in diagnosing and issuing diagnostic reports for a large number of inpatients and outpatients. The average number of patients received daily by this unit is over 110 patients a days for a six working days week. Over 2400 patients are scanned monthly taking most of the clinicians' time in diagnosing and interpreting MRI slices. The dataset was collected using a SIEMENS MAGNETOM Avanto 1.5 Tesla scanner. The provided dataset consists of tumours with different sizes, shapes, locations, orientations and types.

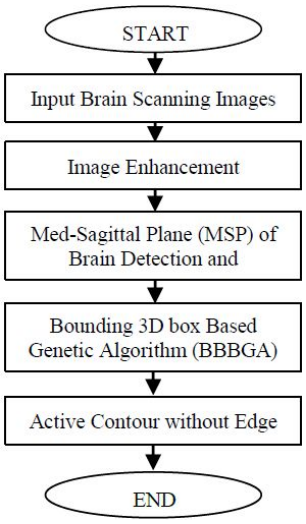

Figure 1: The Flow Chart of the proposed algorithm.

2.2 Image Pre-processing

Two preprocessing steps are performed on the MRI brain scans; image enhancement and MRI intensity normalization due to the intra-scan and inter-scan image intensity variations and Mid-Sagittal Plane detection and correction algorithm (Anju et al., 2013; Lauwers et al., 2010; Aelterman et al., 2008; Bovik, 2009; Nabizadeh and Kubat, 2015).

2.2.1 Unifying the MRI Slices to 512×512

The provided MRI brain slices with a slice resolution of (432×512) pixels and the proposed algorithm in this study is implemented on squared slices of (512×512) pixels. Therefore, the MRI slices are resized by adding extra zeros' columns from left and right till reaching to desired slice resolution.

2.2.2 MRI Image Enhancement

Image enhancement techniques are widely used to refine medical images and improve the visibility of the important structures in medical images. As well as enabling the operators to see the details of the medical image which may not be immediately observable in the original medical image (Bankman, 2000; William, 2001). Generally, the spatial domain techniques are more efficient computationally and require less processing resources for implementation (Gonzalez and Woods, 2002; Birry, 2013). The

Gaussian filter is chosen for noise suppression in this study due to its performance.

2.2.3 Mid-Sagittal Plane Detection and Correction

The Mid-Sagittal Plane (MSP) identification is an important step in brain image analysis as it provides an initial estimation of the brain's pathology assessment and tumour detection (Jayasuriya and Liew, 2012). The human brain is divided into two hemispheres that have approximately a bilateral symmetry around the MSP. This means that most of the structures in one side of the brain have a counterpart on the other side with a similar shape and location. The two hemispheres are separated by the longitudinal fissure that represents a membrane between the left and right hemispheres (Ruppert et al., 2011). The MSP extraction methods can be divided into two groups (Ruppert et al., 2011; Liu, 2009); Content-based methods that are based on finding a plane that maximizes a symmetry measure between both sides of the brain (Christensen et al., 2006; Ardekani et al., 1997; Khotanlou et al., 2009; Ruppert et al., 2011) and shaped-based methods that use the inter-hemispheric fissure as a simple landmark to extract and detect the MSP (Bergo et al., 2009; Liu, 2009).

In this study, we choose to determine the orientation of the patient's head instead of depending on measuring the symmetry to identify the brain MSP as we are using the principal components analysis (PCA) method to compute the distinctive principle axes that are orthogonal to each other. Those axes are used to characterize the patient's head by representing the spatial distribution of the mass (Liu, 2009).

The proposed algorithm includes five steps; the first step separates the brain from the background by using the histogram thresholding approach because the background normally has much higher number of unavailing pixels (Nabizadeh, 2015).

The second step uses holes filling morphological operator to fill the holes that are defined as a background region of a binary image and surrounded by connected borders of foreground (Dougherty, 2009; Bovik, 2009; Soille, 2003; Wilson and Ritter, 2000) as shown in Fig. 2.

The third step determines the orientation of the patient's head using PCA. The PCA method essentially attempts to transfer the coordinate of the original data to a new coordinate system. Such that the maximum variation in the data comes to lie on the first coordinate. This is known as the first principal component. The second maximum variation in the data lies on the second coordinate and so on (Smith, 2002; Wallisch et al., 2014; Manly, 1988).

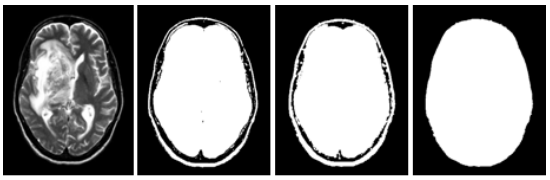

Figure 2: An example for MRI brain scanning image segmentation, A) Original MRI image, B) Segmented MRI image with threshold equal to 25, C) Dilated MRI image, and D) Filled holes image.

The new coordinates of the given data are estimated by calculating the eigenvectors which point in the direction of the new dataset coordinates. The desirable coordinate that has the highest eigenvalues, passes through the maximum variation of data, representing the orientation of the patient's head (Wallisch et al., 2014). The angle θ between the X-axis and X'-axis represents the degree of skewness of the patient's head during the MRI test as shown in Fig. 3 and could be calculated using equation (1):

$$\theta = \tan^{-1}\frac{V_2}{V_1} \quad (1)$$

Where, V_1 and V_2 are the eigenvectors which are related to the maximum eigenvalues.

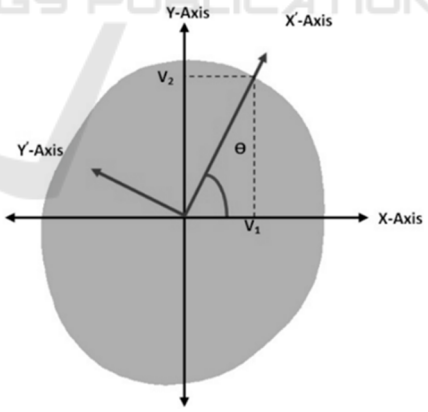

Figure 3: Original and new coordinates of brain.

The fourth step is a Geometrical transformation which is widely used in computer graphic and image analysis. It is used to rotate and correct the patient's head by the computedθ.

The fifth step is the positioning of the patient's head in the centre of the MRI image because identifying the brain's abnormality depends essentially on measuring the symmetry between the

two brain's hemispheres.

The MRI brain slices of each patient have the same degree of skewness therefore the MSP detection and correction algorithm is implemented on a single slice instead of using all slices to avoid computational complexity. The preferable slice for implementing the MSP detection and correction algorithm is the slice which is located in middle of the slices.

2.2.4 Exponential Transformation of MRI Brain Slices

Exponential transformation is the process of compressing the low contrast regions in an MRI brain image and expanding the high contrast region in a non-linear way. It is used to increase the intensity difference between the brain tumour and the surrounded soft tissue (Khandani et al., 2009). This will help the GA to converge and move the generated 3D box faster and accurately to the abnormal region of the brain.

3 BOUNDING 3D BOX BASED GENETIC ALGORITHM

The novel BBBGA is proposed in this study to identify the location of the tumours in MRI brain slices automatically without the need for user interaction. Where, a hundred of 3D boxes with different sizes and locations are randomly generated in the left hemisphere of the brain and these 3D boxes are compared with the corresponding 3D boxes in the right hemisphere of the brain through the objective function. The 3D boxes are optimized and moved using GAs towards the region that maximized the objective function value. The objective function value is high when the 3D boxes stands on the tumour region and low when the 3D boxes stands on the soft tissues because the tumour is always brighter than the soft surrounding tissue of the brain (Khandani et al., 2009). The output of BBBGA is the slices that contain the tumour and corresponds to the optimized 3D box that bounded the tumour over the relevant subset of slices. The BBBGA method does not need image registration nor intensity standardization in MRI slices and is an unsupervised method.

3.1 The Design of the GA

There are several issues involved in designing GAs such as individual size and population size in addition to choosing the most appropriate operations such as selection, crossover and mutation methods.

3.1.1 Individual Construction

As mentioned previously, the provided dataset of MRI brain scanning slices were unified to (512 × 512) pixels dimensions and each patient has 32 slices. The 3D boxes that are generated randomly in the left side of the brain are compared with the corresponding 3D boxes of the right side by using the fitness function. The size of the search space will be (512 × 256 × 32) pixels, and each generated 3D box is defined by six variables that represent the coordinates of the 3D boxes in the search space. Fig. 4 shows the original generated 3D boxes by the GA, such that each generated 3D box in the right hemisphere has a corresponding 3D box in the right hemisphere.

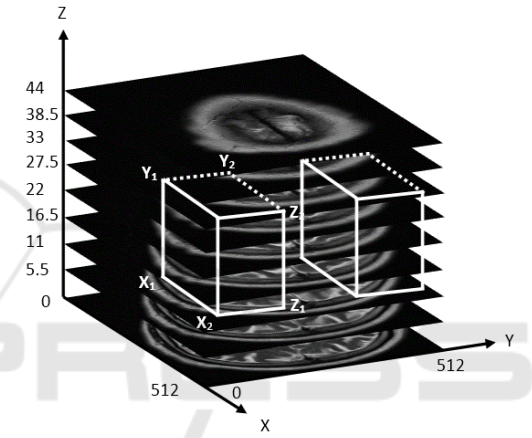

Figure 4: Representation of one 3D box in the brain left hemisphere using (x_1, x_2, y_1, y_2, z_1, z_2) coordinates and opposite region.

Each individual in the GA population denotes the binary representation of the coordinates of one 3D box (x_1, x_2, y_1, y_2, z_1, z_2). Where, x_1 and x_2 represent the height of the 3D box and are subjected to the following constraints; $1 \leq x_1 < 512$ and $x_1 < x_2 \leq 512$. While y_1 and y_2 represent the width of the 3D box and are subjected to the following constraints; $1 \leq y_1 < 256$ and $y_1 < y_2 \leq 256$, and z_1 and z_2 represent the depth of the 3D box and are subjected to the following constraints; $1 \leq z_1 < 31$ and $z_1 < z_2 \leq 32$. Fig. 5 shows how the coordinates of the 3D box (x_1, x_2, y_1, y_2, z_1, z_2) are mapped to the individual of the GA in a binary form where, this individual represents one 3D box with the coordinates (135, 220, 23, 196, 10, 16).

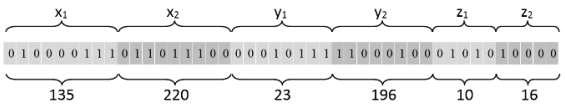

Figure 5: Individual structure.

x_1 and x_2 variables are composed of nine bits as they vary from 1 to 512, while y_1 and y_2 variables are composed of eight bits and vary from 1 to 256 and z_1 and z_2 variables are compose of five bits and vary from 1 to 32. Subsequently, the individual size becomes equal to 44 bits. By using the objective function, we can measure the performance of individuals in the problem domain (Chipperfield et al., 1994). In this study, the fittest individuals that have the highest numerical value of the associated objective function are preserved. The objective function g that is used in this study is based on finding the absolute value of subtracting the means of the intensities inside the generated 3D box in the left hemisphere from the corresponding 3D box in the right hemisphere using equation (2):

$$g = \frac{1}{x, y, z}\left|\sum_{i,j,k}^{x,y,z} I_L(i,j,k) - \sum_{i,j,k}^{x,y,z} I_R(i,j,k)\right| \quad (2)$$

Where x, y and z are the coordinates of the generated 3D box on the left hemisphere and the corresponding opposite region in the right hemisphere.

4 TUMOUR SEGMENTATION USING 3D ACTIVE CONTOUR WITHOUT THE EDGE METHOD

The principle goal of the segmentation process is to partition a medical image into sets of regions. It is an important step in medical image processing and has been used in many medical applications (Bankman, 2000). The Active Contour approach, also known as the Snakes method is the most popular method and was introduced by Kass et al., (1988). It is a very successful approach for image segmentation. It generates a snake or contour within an image domain. The contour can be moved and directed under the effect of internal forces within the same contour and external forces from the image data (Xi-ping et al., 2002). The location of the contour in the given image is associated with the energy function E which is, minimum when the contour reaches the object boundary within the image. Through an iterative process the contour deforms and the associated energy is updated until reaching the minimum value or the maximum number of iteration is reached. In this study, we use the 3D active contour without edge model as proposed by Chan and Vese (2001). This model can detect object boundaries with or without gradient, even when the object boundaries are very smooth or with discontinuity because the main idea of this method is to consider also the information inside the object not only at its boundaries (Rousseau, 2009, Klotz, 2013). To fully segment the tumour, the 3D active contour without edge method is applied on all MRI brain slices of each patient, where the initial contour is defined as a 3-dimensional 3D box inside the desired object and optimally selected by the BBBGA method. The segmentation of all patients were compared with the reference image (manual segmentation) which is segmented by experts, such that the true positive (TP) represents the number of pixels which are correctly segmented, the false positive (FP) represents the number of pixels which are incorrectly segmented, the false negative (FN) represents the number of pixels which are available in the reference image and outside the segmented image by the proposed algorithm, and the true negative (TN) represents the summation of TP, FP and FN rates (Anbeek et al., 2005). The accuracy of segmentation is defined as follows (Nabizadeh and Kubat, 2015):

$$Accuracy = \frac{(TP + TN)}{(TP + TN + FP + FN)} \times 100 \quad (3)$$

5 EXPERIMENTAL RESULTS AND DISCUSSION

To evaluate the proposed algorithms which were proposed in this study a set of examples will be implemented using these algorithms.

5.1 MSP Detection and Correction Results

Fig. 6 shows examples of detecting and correcting the MSP of the brain of three MRI brain scanning images which are oriented with different directions. The MRI brain scanning image is shown in Fig. 7, is re-sampled using the Geometric Rotator system object in MATLAB Image Processing Toolkit (Matlab, 2013), to rotate the patient's head with different yaw angles from -10 to 10 degrees in 5 degree intervals. The proposed algorithm is evaluated by comparing the achievable results with the proposed algorithms in (Liu and Collins, 1996) as shown in Table 1. It is noted that there is a significant difference in the mean squared error (MSE) between the proposed algorithms.

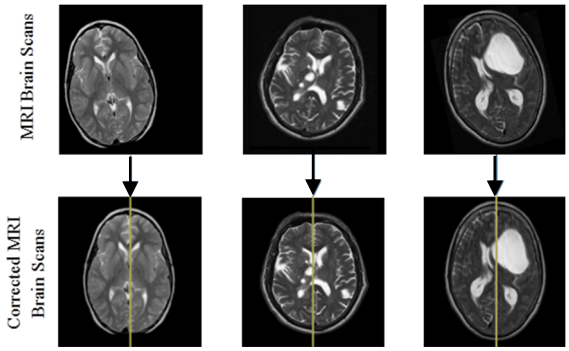

Figure 6: MSP detection and correction of three pathological patients.

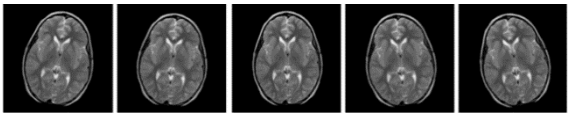

Figure 7: Re-sampling of one slice from the axial MRI brain scanning image with varied rotate angles.

Table 1: Numerical results of detecting yaw angle.

Yaw Angle	-10	-5	0	5	10	MSE
Computed Yaw Angle	-9.1	-4.7	0.5	5.4	10.5	0.3
(Liu and Collins, 1996)	-8.5	-3	1.25	6.5	11.2	2.87

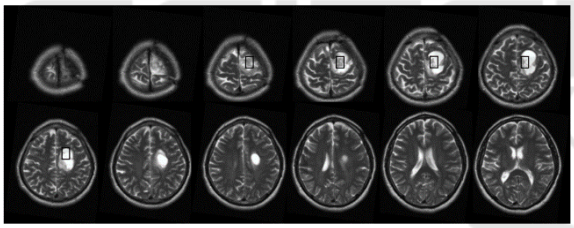

Figure 8: MRI brain scanning slices.

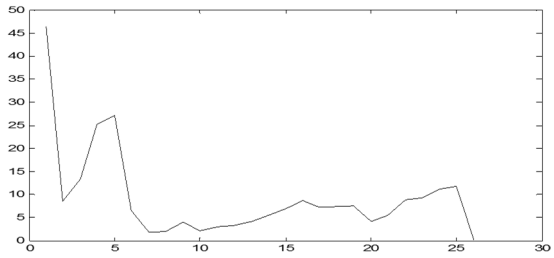

Figure 9: RMSE over 27 iterations by GA.

Once the patient's head is corrected, we apply the BBBGA method to localize the brain tumour. Fig. 8 shows the output of BBBGA implementation on MRI brain scanning slices of pathological patient with a population size equal to 100 and a mutation rate equal to 0.05. The optimal selected slices are 3 to 7. Fig. 9 shows how the RMSE decreases to the minimum value within 27 iterations of GA. The achievable accuracy by BBBGA was 95%, such that, there were only 4 cases where the system has failed to identify the abnormality because of the tumour's size is less than 1 cm^3.

5.2 Tumour Segmentation Results

Fig. 10 shows the result of segmentation of a pathological patient, who has a brain tumour starting from slice 2 and ending in slice 9. The MRI scans in the dataset are manually segmented by expert and the achievable segmentation accuracy was 90±3.7% by 3D Active Contour without Edge method. The same dataset was segmented by 2D Active Contour without Edge method and the achievable accuracy was 86.9±3.7%. Fig. 11 shows a comparison between the 3D and 2D segmentation of given dataset, such that it is noted that the 3D segmentation outweighs the 2D segmentation for all patients in the given dataset. Subsequently, it is possible to identify the most relevant slices to draw the attention of the clinicians about these slices instead of spending long time on diagnosing and interpreting MRI slices. Fig. 12 shows a comparison of identifying clinically and experimentally the most relevant slices for the provided pathological patients after segmentation. We have test the null hypothesis to prove that there is no significant difference was found between automatic and manual identification of slices showing the tumor (t-test, p=0.86).

6 CONCLUSION

This paper presented an automated system that is able to detect the location of tumour and then segment it automatically in addition to identifying the most relevant slices that should be diagnosed by clinicians without requiring to inspect all patients' slices.

The BBBGA method exploits the symmetry feature of axial viewing of MRI brain slices to search about the most dissymmetry region in the brain, additionally it is unsupervised method meanwhile it does need for training phase and it does not need for image registration.

A major difficulty of segmentation with a white matter tumours because of overlapping of the intensity distributions of the white and grey matter. As well as, some parts of the tumours in the grey matter cannot be distinguished due to finite resolution of the images and complicated shapes of the brain tissues that impact on a large number of the voxels which are located on the borders of tissues. In addition, image intensity in the centre of tumour is

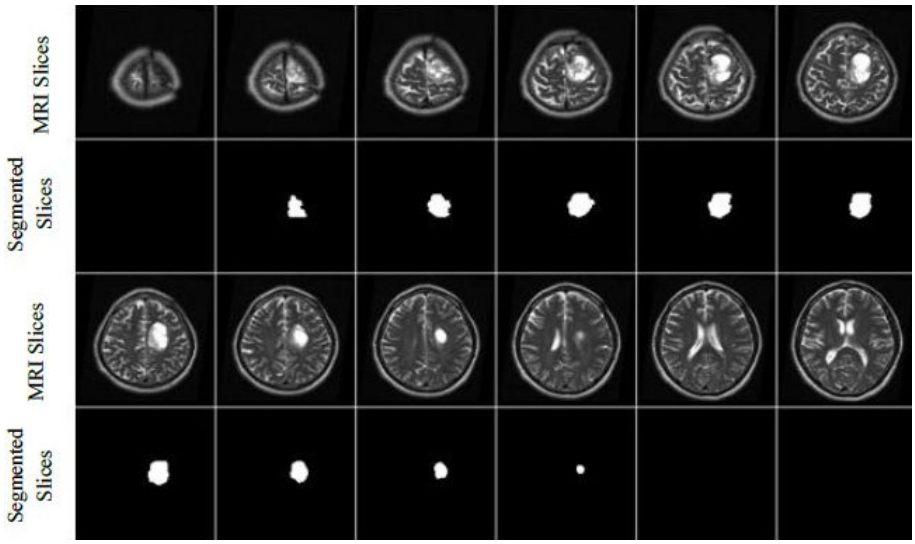

Figure 10: The result of segmentation of T2 weighted MRI brain slices by3D active contour without edge segmentation method.

different from its Periphery. Therefore, the image intensity at the borders of tumour may be the same as grey matter. This phenomenon may cause confusion between grey matter and tumours and result in misclassification of the peripheral regions of the tumours, which is occurred in T2 weighted.

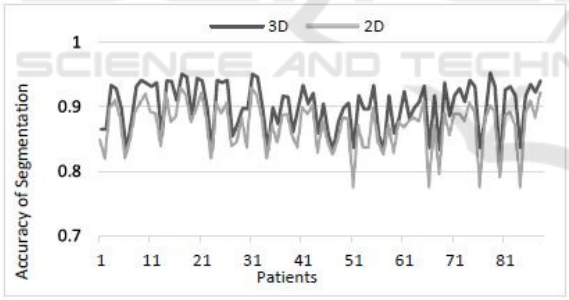

Figure 11: Comparison between 3D and 2D segmentation for given dataset.

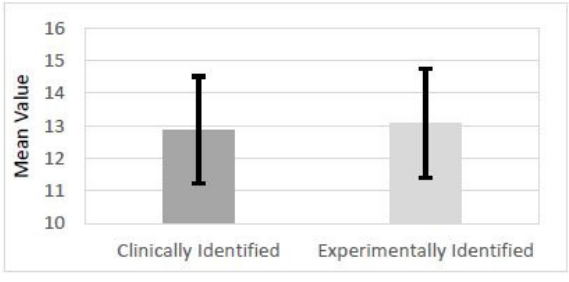

Figure 12: Comparison between clinically and experimentally MRI slice identification.

ACKNOWLEDGEMENTS

We would like to thank the MRI Unit in Al Kadhimiya Teaching Hospital in Iraq for providing us the diagnosed dataset of MRI brain scanning images.

REFERENCES

Aelterman, J., Goossens, B., Pizurica, A. & Philips, W. 2008. Removal of correlated rician noise in magnetic resonance imaging. *16th European Signal Processing Conference.* Switzerland.

Anbeek, P., Vincken, L., Van Bochove, S., Van Osch, P. & Van Der Grond, J. 2005. Probabilistic segmentation of brain tissue in MR imaging. *NeuroImage,* 27**,** 795-804.

Anju, E., Karnan, M. & Sivakumar, R. 2013. MR brain image classification with supervised bacteria foraging technique using SVM. *International Journal of Futuristic Science Engineering and Technology,* 1**,** 318-322.

Ardekani, A., Kershaw, J., Braun, M. & Kanno, I. 1997. Automatic detection of the mid-sagittal plane in 3-D brain images. *IEEE Trans Med Imaging,* 16**,** 947-52.

Bankman, I. (ed.) 2000. *Handbook of medical imaging*: Academic Press, Inc.

Bauer, S., Nolte, L. & Reyes, M. 2011. Fully Automatic Segmentation of Brain Tumor Images using Support Vector Machine Classication in Combination with hierarchical Conditional Random Field Regularization. *Medical Image Computing and Computer-Assisted Intervention-Springer Berlin Heidelberg***,** 354-361.

Bergo, F., Falcão, A., Yasuda, C. & Ruppert, G. 2009. Fast, Accurate and Precise Mid-Sagittal Plane Location in

3D MR Images of the Brain. *Biomedical Engineering Systems and Technologies.* Springer Berlin Heidelberg.

Birry, R. 2013. *Automated Classification in Digital Images of Osteogenic differentiated stem Cells.* PhD, University of Salford, Manchester.

Bovik, A. 2009. *The Essential Guide to Image Processing,* Elsevier Inc.

Chan, F. & Vese, A. 2001. Active contours without edges. *Image Processing, IEEE Transactions,* 10**,** 266-277.

Chipperfield, A., Fleming, P., Pohlheim, H. & Fonseca, C. 1994. *Genetic Algorithm TOOLBOX for Use with MATLAB*.

Christensen, J., Hutchins, G. & Mcdonald, C. 2006. Computer automated detection of head orientation for prevention of wrong-side treatment errors. *AMIA Annu Symp Proc***,** 136-40.

Dougherty, G. 2009. *Digital Image Processing for Medical Applications*.

Gonzalez, R. & Woods, R. 2002. *Digital Image Processing.*

Jayasuriya, S. & Liew, A. 2012. Symmetry plane detection in neuroimages based on intensity profile analysis. *Information Technology in Medicine and Education (ITME), International Symposium on.* Australia IEEE.

Kaal, E. C. & Vecht, C. J. 2004. The management of brain edema in brain tumors. *Current opinion in oncology,* 16**,** 593-600.

Kass, M., Witkin, A. & Terzopoulos, D. 1988. Snake: Active Contour Models. *International Journal of Computer Vision,* 1**,** 321-331.

Khandani, M., Bajcsy, R. & Fallah, Y. 2009. Automated Segmentation of Brain Tumors in MRI Using Force Data Clustering Algorithm. *Advances in Visual Computing.* Springer Berlin Heidelberg.

Khotanlou, H., Colliot, O., Atif, J. & Bloch, I. 2009. 3D brain tumor segmentation in MRI using fuzzy classification, symmetry analysis and spatially constrained deformable models. *Fuzzy Sets and Systems,* 160**,** 1457-1473.

Klotz, A. 2013. *2D and 3D multiphase active contours without edges based algorithms for simultaneous segmentation of retinal layers from OCT images.* MS.c, University of Texas at Austin.

Lauwers, L., Barbé, K., Van Moer, W. & Pintelon, R. 2010. Analyzing Rice distributed functional magnetic resonance imaging data: a Bayesian approach. *Measurement Science and Technology,* 21**,** 115804.

Liu, S. 2009. Symmetry and asymmetry analysis and its implications to computer-aided diagnosis: A review of the literature. *Journal of Biomedical Informatics,* 42**,** 1056-1064.

Liu, Y. & Collins, R. 1996. Automatic Extraction of the Central Symmetry (MidSagittal) Plane from Neuroradiology Images. Robotics Institute, Carnegie Mellon University.

Manly, B. 1988. *Multivariate Statistical Methods A primer,* Department of mathematics and statistics, university of Otago.

Matlab 2013. The Math Works kit.

Mikulka, J. & Gescheidtov, E. 2013. An Improved Segmentation of Brain Tumor, Edema and Necrosis. *Progress In Electromagnetics Research Symposium Proceedings, Taipei.*

Nabizadeh, N. 2015. *Automated Brain Lesion Detection and Segmentation Using Magnetic Resonance Images.* PhD, University of Miami.

Nabizadeh, N. & Kubat, M. 2015. Brain tumors detection and segmentation in MR images: Gabor wavelet vs. statistical features. *Computers & Electrical Engineering*.

Ray, N., Greiner, R. & Murtha, A. 2008. Using Symmetry to Detect Abnormalies in Brain MRI. *Computer Society of India Communications,* 31**,** 7-10.

Rousseau, O. 2009. *Geometrical Modeling of the Heart.* Ph.D, University of Ottawa.

Ruppert, G., Teverovskiy, L., Chen-Ping, Y., Falcao, X. & Yanxi, L. A new symmetry-based method for mid-sagittal plane extraction in neuroimages. Biomedical Imaging: From Nano to Macro, International Symposium on, 2011 Chicago, IL. IEEE, 285-288.

Shen, S., Sandham, W., Granat, M. & Sterr, A. 2005. MRI fuzzy segmentation of brain tissue using neighborhood attraction with neural-network optimization. *Information Technology in Biomedicine, IEEE Transactions on,* 9**,** 459-467.

Smith, L. 2002. A tutorial on Principal Components Analysis.

Soille, P. 2003. *Morphological Image Analysis: Principles and Applications*, Springer-Verlag New York, Inc.

Wallisch, P., Lusignan, M., Benayoun, M., Baker, T., Dickey, A. & Hatsopoulos, N. 2014. *Matlab for Neuroscientists*, Elsevier.

William, K. 2001. *Digital Image Processing,* Canada, Wiley-Interscience.

Wilson, J. & Ritter, G. 2000. *Handbook of Computer Vision Algorithms in Image Algebra*, CRC Press, Inc.

Xi-Ping, L., Jie, T. & Yao, L. 2002. An Algorithm for Segmentation of Medical Image Series Based on Active Contour Model. *Journal of Software,* 13**,** 1050-1058.